

Single image dehazing using image boundary constraint and nearest neighborhood optimization

Sidharth Gautam
Indian Institute of Technology
New Delhi, India
eez158415@ee.iitd.ac.in

Tapan Kumar Gandhi
Indian Institute of Technology
New Delhi, India
tgandhi@ee.iitd.ac.in

B.K.panigrahi
Indian Institute of Technology
New Delhi, India
bkpanigrahi@ee.iitd.ac.in

ABSTRACT

Single image dehazing is an ill-posed problem that requires assumptions, priors and constraints to solve. In this paper, boundary constraint utilizing median filter has been proposed on the image radiance for the rough estimation of transmission-map in haze images. Furthermore, for the refinement of estimated transmission-map, the proposed method use a multi-dimensional feature space that uses nearest neighborhood optimization under the framework of non-local principle. Experimental results manifest that proposed method is effective and results in visually appealing dehaze images that can be useful for subsequent user or computer based application.

CCS CONCEPTS

- Computing methodologies → Reconstruction;

ACM Reference Format:

Sidharth Gautam, Tapan Kumar Gandhi, and B.K.panigrahi. 2018. Single image dehazing using image boundary constraint and nearest neighborhood optimization. In *11th Indian Conference on Computer Vision, Graphics and Image Processing (ICVGIP 2018), December 18–22, 2018, Hyderabad, India*, Anoop M. Namboodiri, Vineeth Balasubramanian, Amit Roy-Chowdhury, and Guido Gerig (Eds.). ACM, New York, NY, USA, Article 78, 5 pages. <https://doi.org/10.1145/3293353.3293431>

1 INTRODUCTION

In recent years there is an increasing interest in vision and graphics communities to dehaze images by using a minimal input (i.e. single image). Under inclement weather conditions, when images are captured by digital devices, light after reflecting from an object is absorbed and scattered in the atmosphere before it reaches the camera. This is due to the particles suspended in the air in the form of dust, smoke, and haze. These particles results in ‘direct-attenuation’ and ‘air-light contribution’ [1], which play their role collectively, to degrade the visibility and contrast of an image. Thus, it is desired to develop an effective restoration technique that can dehaze images and recovers perceptual image quality for computer vision application used for object recognition, tracking, and navigation.

Permission to make digital or hard copies of all or part of this work for personal or classroom use is granted without fee provided that copies are not made or distributed for profit or commercial advantage and that copies bear this notice and the full citation on the first page. Copyrights for components of this work owned by others than ACM must be honored. Abstracting with credit is permitted. To copy otherwise, or republish, to post on servers or to redistribute to lists, requires prior specific permission and/or a fee. Request permissions from permissions@acm.org.

ICVGIP 2018, December 18–22, 2018, Hyderabad, India

© 2018 Association for Computing Machinery.

ACM ISBN 978-1-4503-6615-1/18/12...\$15.00

<https://doi.org/10.1145/3293353.3293431>

A method that has been explored in recent years for single image dehazing is proposed by He et al.[2] and known as dark channel prior (i.e. DCP). Although, the DCP technique is able to achieve nice dehazing results, but it is very time consuming and thereby limiting their application in real-time dehazing. Furthermore, it also features halo-artefacts around complex-structures and sky-regions in haze images. To overcome the shortcomings of DCP, some improved algorithm have been proposed in [3]-[15]. To speed up the dehazing, Tripathi et al. [4] replace the time consuming soft-matting with anisotropic-diffusion, but the method often results in inferior performance compared to He et al.[2]. Similarly, Meng et al. [5] developed a regularization based dehazing technique for single images. This method over-estimates the haze contribution and therefore, produce saturated images. Baig et al. [6] improves the Meng et al. [5] method, using quad tree decomposition and entropy based weighted regularization.

Zhu et al. [7] used machine learning approach to model the scene depth and creates color-attenuation-prior (i.e. CAP). This prior estimate the haze contribution by calculating the difference between image brightness and saturation component. Although, the method is fast owing to the use of guided filter, but its performance depends on the accuracy of estimated scene transmission, which is difficult to achieve when the prior becomes invalid.

Tang et al. [8] use haze-relevant features such as dark channel, hue disparity, local max saturation, local max contrast, and then employed random forest to learn the correlation between haze-relevant features and medium transmission. This method often produce poor dehazing results as these features are not efficient enough. Fattal et al. [9] estimate the transmission in haze images using the concept of color-line. This method is based on the observation that haze environment fades the local colors of the image, and shift them towards air-light. Cai et al. [10] dehaze images using machine learning framework and develop dehazenet that uses CNN for the transmission-map estimation. Berman et al. [11] improve the dehazing using a non-local method, where colors of a haze image form clusters in the RGB space. These cluster are then used to form haze-lines for the estimation of transmission of different pixels.

Besides the above dehazing methods, many other interesting dehazing algorithms were also proposed such as [12],[13],[14],[15]. The most recent work is proposed by Bui et al. [12], which uses color ellipsoid prior for dehazing.

The remainder of the paper is organized as follows. We review a brief background of optical model in section II, followed by description of DCP approach. Our dehazing approach is detailed in section III. Experimental results are discussed in section IV. Finally, concluding remarks are provided in section V.

2 BACKGROUND

In this section, we will briefly discuss the optical model and dark channel prior used for the dehazing of outdoor images.

2.1 Optical model

The optical model [1]-[15] widely used to describe the formation of hazy images, is described as follows:

$$I(x) = J(x)t(x) + a_{ir}(1 - t(x)) \quad (1)$$

$$t(x) = e^{-\beta d(x)} \quad (2)$$

where, $I(x)$ is the intensity of observed haze image, $J(x)$ is the radiance of haze-free image, a_{ir} is the global air-light, $t(x)$ is the medium transmission-map. The transmission-map $t(x)$ is a function of atmospheric attenuation coefficient (β) and distance $d(x)$ between the camera and the scenery object. On putting the value of $t(x)$ in Eq. (1):

$$I(x) = J(x)e^{-\beta d(x)} + a_{ir}(1 - e^{-\beta d(x)}) \quad (3)$$

In Eq. (3), $J(x)e^{-\beta d(x)}$ is called ‘direct attenuation’ which exponentially reduce the scene radiance in proportional to the distance, and $a_{ir}(1 - e^{-\beta d(x)})$ is called the ‘local air-light’ which fades the color and adds whiteness in the scene. Intuitively, the image received by the observer is the combination of the attenuated version of underlying scene radiance with an additive air-light. Since $I(x)$ is known, the ultimate goal of dehazing is to recover $J(x)$, as:

$$J(x) = \frac{I(x) - a_{ir}}{e^{-\beta d(x)}} + a_{ir} \quad (4)$$

The restoration of scene radiance $J(x)$, is a highly ill-posed inverse problem, because it requires us to recover a_{ir} and $t(x)$, using only a single image $I(x)$. In order to find the solution of this ill-posed problem, we need to rely on some constraints, priors, and assumptions.

2.2 Dark channel prior

The DCP [2] is based on the property of “dark pixels”, which have very low intensity in at least one color channels of an outdoor haze-free images. Mathematically, the DCP for a haze-free image $J(x)$ is calculated as follows:

$$J^{Dark}(x) = \min_{y \in \Omega_r(x)} \left(\min_{c \in \{r, g, b\}} J^c(y) \right) \quad (5)$$

where, x and y represents the pixels locations, $\Omega_r(x)$ represents an $(r \times r)$ local patch centered at x , J^c is the c^{th} color-channel, $c \in \{r, g, b\}$, and \min is a minimum filter.

2.3 Estimation of transmission-map

For the estimation of transmission-map $t(x)$, it is assumed that air-light (a_{ir}) is given and the value of $t(x)$ in a local-patch $\Omega_r(x)$ is constant. On calculating the DCP value on both side of Eq. (1), and normalized by (a_{ir}), we have:

$$\min_{y \in \Omega_r} \left(\min_c \left(\frac{J^c(y)}{a_{ir}^c} \right) \right) = \min_{y \in \Omega_r} \left(\min_c \left(\frac{J^c(x)}{a_{ir}^c} \right) \right) \tilde{t}(x) + 1 - \tilde{t}(x) \quad (6)$$

According to the DCP [2], the dark channel of $J(x) \approx 0$

$$\min_{\Omega_r} \left(\min_c \left(\frac{J^c(x)}{a_{ir}^c} \right) \right) = 0 \quad (7)$$

On putting Eq.(7) into Eq. (6), we have:

$$\tilde{t}(x) = 1 - \min_{\Omega_r} \left(\min_c \left(\frac{J^c(x)}{a_{ir}^c} \right) \right) \quad (8)$$

In order to keep the natural appearance after dehazing, He et al. [2] used a constant w ($0 < w \leq 1$) into Eq.(8) as:

$$\tilde{t}(x) = 1 - w \left\{ \min_{\Omega_r} \left(\min_c \left(\frac{J^c(x)}{a_{ir}^c} \right) \right) \right\} \quad (9)$$

where, w is set to 0.95. The abrupt transitions in $\tilde{t}(x)$ can be smoothed out through a soft-matting technique[16] as optimal transmission $t(x)$ and used in Eq.(4) for radiance recovery.

2.4 Discussion

Despite good performance, the DCP has few limitations as:

2.4.1 Small patch size: The DCP shows good dehazing results when the local color distribution in the background and foreground region of an image are non-overlapped. But this theory fails, especially, when an image local-color blends with air-light. Therefore, to relieve the problem and to satisfy the assumption of color-model, the patch size $\Omega_r(x)$ kept unavoidably small in DCP.

2.4.2 Inefficient transmission estimation: Eq. (9) leads to the false estimation of transmission-map $\tilde{t}(x)$, especially when intensity of any bright object in haze images becomes similar to the intensity of air-light (a_{ir}) as:

$$\min_{\Omega_r} \left(\min_c \left(\frac{J^c(x)}{a_{ir}^c} \right) \right) \rightarrow 1 \quad \text{and} \quad \tilde{t}(x) \rightarrow 0 \quad (10)$$

Eq. (10) implies that DCP fails to obtain the scene transmission, which is the key for efficient dehazing. Furthermore, the use of \min operator in Eq. (9) discard the edges information, sharply decrease the image resolution and therefore, results in a blurry transmission-map.

3 PROPOSED METHOD

In this paper, we propose a dehazing scheme using boundary constraint and nearest neighborhood optimization.

3.1 Estimation of air-light

For the air-light estimation, we use He et al. [2] approach as:

- (a) First, calculate the DCP of a haze image using Eq. (5).
- (b) Second, select the top 0.1% brightest pixels in DCP.
- (c) Third, select the pixels with *max* intensity in haze-image (I) as air-light (a_{ir}).

3.2 Estimation of transmission-map

In order to find an initial estimate of transmission-map $t(x)$, we can rewrite Eq. (1) as:

$$J(x) = \frac{I(x) - a_{ir}(1 - t(x))}{t(x)} \quad (11)$$

To impose the boundary constraint, it is assumed that the normalized intensity of each color channel is within the range [0, 1].

$$0 \leq \frac{I^c(x) - a_{ir}^c(1 - t(x))}{t(x)} \leq 1 \quad (12)$$

The solution of Eq. (12) results in the two equations as:

$$t_1(x) \geq 1 - \frac{I^c(x)}{a_{ir}^c} \quad \text{and} \quad t_2(x) \geq \frac{I^c(x) - a_{ir}^c}{1 - a_{ir}^c} \quad (13)$$

The initial estimation of transmission-map $t_i(x)$ can be given by:

$$t_i(x) = \max \{t_1(x), t_2(x)\} \quad (14)$$

The transmission-map in a local neighborhood (Ω) is obtained via:

$$\hat{t}(x) = \operatorname{med}_{y \in \Omega_r(x)} \left(\max_{z \in \Omega_r(y)} (t_i(z)) \right) \quad (15)$$

where, $\Omega_r(x)$ and $\Omega_r(y)$ represent an image $(r \times r)$ local patch centered at pixel location x and y , respectively. The *med* operator in Eq. (15) avoids to decrease the perceptible resolution sharply unlike in [2] and performs a non-linear filtering operation, which not only suppresses the noise, but also preserves the edges, while estimating the transmission-map.

3.3 Transmission-map refinement

The rough estimation of transmission-map $\hat{t}(x)$ contains inter-region transitions, which may produce block-artefacts, if the same $\hat{t}(x)$ is used for the $J(x)$ recovery. Hence, it is necessary to refine the $\hat{t}(x)$, so that we can smoothed out the abrupt transition. The method used for the refinement of $\hat{t}(x)$ is motivated by the assumption that pixels sharing the same appearance must share the same transmission value [17]. Therefore, to measure the similarity, we developed a 9-dimensional feature space, which uses spatial variations, and edges variations as an additional feature to color as:

$$\phi_x = \left[p \ q \ h \ s \ v \ |I_p| \ |I_q| \ |I_{pp}| \ |I_{qq}| \right]_x \quad (16)$$

where, $I = [h, s, v]$ represents the pixels value in the HSV color space, (p, q) represents the spatial coordinates of pixel (x) . I_p , I_q , I_{pp} , and I_{qq} represent the first and second-order derivative of image intensity in the horizontal and vertical directions. To enforce the inter-region smoothness in $\hat{t}(x)$, a pixel (x) is connected to its K -nearest neighbors y_1, y_2, \dots, y_K with weights[18] as:

$$w(x, y) = 1 - \frac{\sum_{x=1}^N \|\phi_x - \sum_{m=1}^K \phi_{ym}\|}{\sigma} \quad (17)$$

where, y is a neighboring pixel of x , N is the total number of pixels, σ is the least upper bound $\sum_{x=1}^N \|\phi_x - \sum_{m=1}^K \phi_{ym}\|$ to make values of $w(x, y)$ in $[0, 1]$. The refined transmission-map $t(x)$ is obtained by minimizing the following cost function:

$$E = \xi \sum_{x \in V} (t_x - \hat{t}_x)^2 + \sum_{x=1}^N \left(\sum_{y \in N_x} w_{xy} (t_x - \hat{t}_x)^2 \right) \quad (18)$$

Here, the first term ensures that the refined transmission-map $t(x)$ is consistent with the constraint of $\hat{t}(x)$, whereas the second term ensures that the neighboring pixels must share similar transmission values, ξ is a parameter to keep the balance between these two terms. Here, V represents a set of pixels whose initial transmission estimation (\hat{t}) is of high confidence, and N_x is the set of neighbor of pixels x . To facilitate computation, we can rewrite Eq. (18) as:

$$E = \xi (t - \hat{t})^T \Gamma (t - \hat{t}) + t^T L^T L t \quad (19)$$

where,

$$L_{xy} = \begin{cases} w_{xx} & \text{if } x = y \\ -w_{xy} & \text{if } x \text{ and } y \text{ are neighbors} \\ 0 & \text{otherwise} \end{cases}$$

where, $w_{xx} = \sum_{y \in N_x} w_{xy}$, Γ is a $N \times N$ diagonal matrix with $\Gamma_{xx} = 1$ if $x \in V$, else 0. The optimal solution of Eq. (19) is obtained by solving the following sparse linear system [19]:

$$t = (L^T L + \xi U)^{-1} \hat{t} \quad (20)$$

where, U is an identity matrix of same size as L . An example of transmission-map refinement is shown in Fig. 1. The estimated transmission of a haze image is shown in Fig.1 (b), which leads to halo-artifacts while dehazing (see Fig.1 (c)). In Fig.1 (d), we can observe that the irregularities formed while estimating scene transmission are suppressed and smoothed out effectively, which leads to the efficient dehazing and recovery of true scene radiance.

3.4 Image recovery

Once the air-light (a_{ir}) and transmission-map $t(x)$ are obtained, we can recover the scene radiance $J(x)$ by using:

$$J^c(x) = \frac{I^c(x) - a_{ir}^c}{[\min\{\max\{t(x), 0.1\}, 0.9\}]^\delta} + a_{ir}^c \quad (21)$$

For avoiding instability, we also restrict the value of the transmission-map $t(x)$ between 0.1 and 0.9. An exponent parameter δ is also used for the fine detailing of dehazing effects.

4 EVALUATION AND RESULTS

In experiment, we validate the performance of proposed method on outdoor haze images. The proposed method was implemented in Matlab R2017b and was simulated on a PC with Intel(R) Core(TM) i7-3770 CPU@ 3.40GHz, 3401 MHz, 4 Core(s), 8.00GB RAM. The parameter r , k , ξ , and δ are fixed as 15, 12, 10^{-4} and 0.7 in our experiment. The qualitative comparison of dehazing results on few real-world haze images with other state-of-the-art methods are shown in Fig. 2. To do a fair comparison, we disabled the complex post-processing enhancement operations, due to which the reported results might be slightly different from others. The reader is urged to zoom into the pdf file to view the images more carefully. Upon zooming, one can observe, most of the haze effects are removed by [2], [5], [7], [10], and [11] respectively. But visibility, colors, and details are not good enough. It can be seen that in Fig. 2(b), He et al. [2] results significantly suffer from darkness and edge-distortions (i.e. for the swan image, background wall is hard to be seen). Likewise, for the hostel image, bricks and leaves appears much darker than it should be. Similarly, for the logo image, one can observe that fonts are distorted. Meng et al. [5] method produce over-enhanced results due to the over-estimation of haze thickness (see Fig. 2(c)). Zhu et al. [7] avoid the over-enhancement, but final results still appear hazy and distorted (i.e. background wall in the swan image appears hazy, while fonts appears distorted in the logo image). Cai et al. [10] results show similar dehazing limitations as Zhu et al. [7] in Fig.2 (e). The Berman et al. [11] method is able to produce sharp dehazing results, but it also produce color-shifts (i.e. see the swan and tree in the first image, and fonts in the third image). In contrast, our proposed method is able to dehaze image well and restores the natural visibility of the scene.

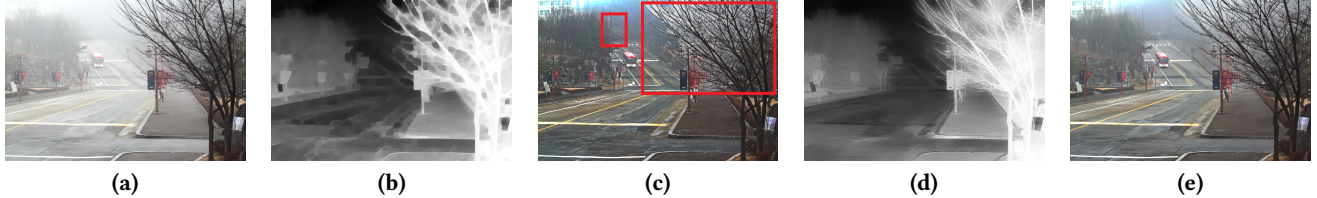


Figure 1: An example of transmission-map refinement using proposed approach. (a) Real haze image. (b) Estimated transmission-map. (c) Dehazing result without transmission-map refinement. (d) Refined transmission-map. (e) Final dehazing result. (Best viewed on high-resolution display with zoom-in).

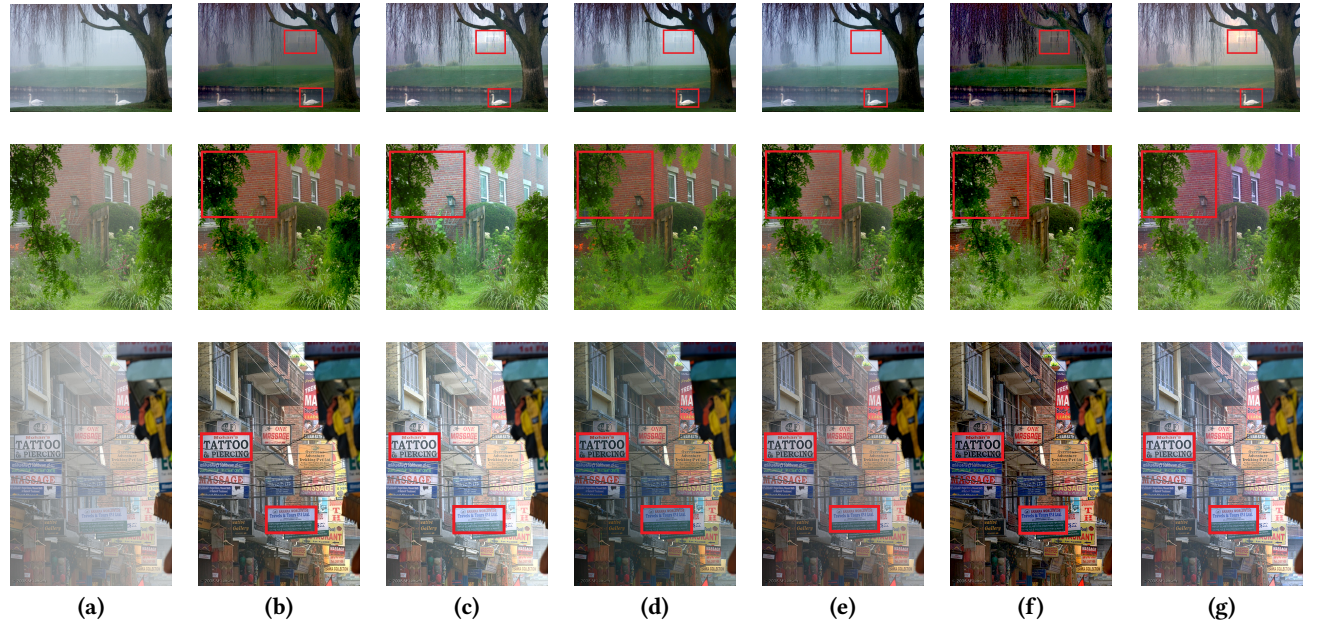


Figure 2: Qualitative comparison of dehazing results with other state-of-the-art methods. (a) Real haze images. (b) He et al. [2] (c) Meng et al. [5] (d) Zhu et al. [7] (e) Cai et al. [10] (f) Berman et al. [11] (g) Our proposed method. (Best viewed on high-resolution display with zoom-in).

Table 1: Dehazing efficacy of the compared methods obtained via Q_e , Q_g and Q_o [20]

Image	Metric	He et al. [2]	Meng et al. [5]	Zhu et al. [7]	Cai et al. [10]	Berman et al. [11]	Ours
Swan	Q_e	0.30	0.35	0.27	0.20	0.42	0.51
	Q_g	1.56	1.60	1.09	1.20	2.13	2.45
	Q_o	0.00	0.00	0.02	1.59	<u>6.20</u>	0.00
Hostel	Q_e	0.28	0.11	0.18	0.16	0.21	0.44
	Q_g	1.30	1.38	0.97	1.08	2.01	4.63
	Q_o	0.00	0.00	0.00	0.92	<u>2.62</u>	0.00
Logo	Q_e	0.24	0.23	0.27	0.24	0.09	0.44
	Q_g	1.16	1.87	1.44	1.54	2.50	1.43
	Q_o	0.01	0.00	0.12	1.66	<u>3.85</u>	0.00

Bold values indicate the efficient dehazing results, whereas underscore value marks the inferior dehazing results.

To evaluate the dehazing efficacy of each compared method, we adopted three well known quantitative metrics- Q_e , Q_g and Q_o [20]. Specifically, the Q_e metric calculates the ratio of visible edges between the dehazed image and the hazy image. Since the dehazed images tends to have sharper details than the hazy image, it is considered that the higher the Q_e value the better the efficacy.

The Q_g metric precisely measure the sharpness, and calculates the average gradient before and after dehaze images. Similarly, higher the Q_g value, better the efficacy. Finally, the Q_o metric estimates the ratio in which the visible edges of the dehaze image are saturated as white or smeared as black. As Q_o accounts for the saturation, the smaller the Q_o value, the better the dehazing results. Table-1

summarizes the dehazing results for images shown in Figure 2. From this table, it can be observed that both Cai et al. [10] method and Berman et al. [11] method dehaze images by producing maximum value of Q_o , among the compared methods. The performance of proposed method is competent as it significantly improves image visibility, while preserving the natural appearance.

5 CONCLUSION

In this paper, we have addressed the inverse problem of dehazing in outdoor images and develop a novel approach that uses median filter inspired boundary constraint on the scene radiance for the rough estimation of transmission-map in haze images. In addition, proposed method uses a 9-dimensional feature space, where spatial variation and edges variation is used as an additional feature to color for the refinement of transmission-map under the framework of non-local principle. Experimental results with the state-of-the-art methods demonstrate that the proposed method effectively distinguish dehazing effects, without causing any visible artifact, and results in overall improvement in image visibility (in terms of both the visual effect and quantitative assessment) than previous dehazing methods in literature. In future works, we will explore our method for video dehazing.

REFERENCES

- [1] S. G. Narasimhan and S. K. Nayar, “Vision and the atmosphere,” *International Journal of Computer Vision*, vol. 48, pp. 233–254, Jul 2002.
- [2] K. He, J. Sun, and X. Tang, “Single image haze removal using dark channel prior,” *IEEE Transactions on Pattern Analysis and Machine Intelligence*, vol. 33, pp. 2341–2353, Dec 2011.
- [3] K. B. Gibson, D. T. Vo, and T. Q. Nguyen, “An investigation of dehazing effects on image and video coding,” *IEEE Transactions on Image Processing*, vol. 21, pp. 662–673, Feb 2012.
- [4] A. K. Tripathi and S. Mukhopadhyay, “Single image fog removal using anisotropic diffusion,” *IET Image Processing*, vol. 6, pp. 966–975, October 2012.
- [5] G. Meng, Y. Wang, J. Duan, S. Xiang, and C. Pan, “Efficient image dehazing with boundary constraint and contextual regularization,” in *2013 IEEE International Conference on Computer Vision*, pp. 617–624, Dec 2013.
- [6] N. Baig, M. M. Riaz, A. Ghafoor, and A. M. Siddiqui, “Image dehazing using quadtree decomposition and entropy-based contextual regularization,” *IEEE Signal Processing Letters*, vol. 23, pp. 853–857, June 2016.
- [7] Q. Zhu, J. Mai, and L. Shao, “A fast single image haze removal algorithm using color attenuation prior,” *IEEE Transactions on Image Processing*, vol. 24, pp. 3522–3533, Nov 2015.
- [8] K. Tang, J. Yang, and J. Wang, “Investigating haze-relevant features in a learning framework for image dehazing,” in *2014 IEEE Conference on Computer Vision and Pattern Recognition*, pp. 2995–3002, June 2014.
- [9] R. Fattal, “Dehazing using color-lines,” *ACM Trans. Graph.*, vol. 34, pp. 13:1–13:14, Dec. 2014.
- [10] B. Cai, X. Xu, K. Jia, C. Qing, and D. Tao, “Dehazenet: An end-to-end system for single image haze removal,” *IEEE Transactions on Image Processing*, vol. 25, pp. 5187–5198, Nov 2016.
- [11] D. Berman, T. Treibitz, and S. Avidan, “Non-local image dehazing,” in *2016 IEEE Conference on Computer Vision and Pattern Recognition (CVPR)*, pp. 1674–1682, June 2016.
- [12] T. M. Bui and W. Kim, “Single image dehazing using color ellipsoid prior,” *IEEE Transactions on Image Processing*, vol. 27, pp. 999–1009, Feb 2018.
- [13] W. Ren, S. Liu, H. Zhang, J. Pan, X. Cao, and M.-H. Yang, “Single image dehazing via multi-scale convolutional neural networks,” 10 2016.
- [14] K. Nishino, L. Kratz, and S. Lombardi, “Bayesian defogging,” *International Journal of Computer Vision*, vol. 98, pp. 263–278, Jul 2012.
- [15] C. O. Ancuti and C. Ancuti, “Single image dehazing by multi-scale fusion,” *IEEE Transactions on Image Processing*, vol. 22, pp. 3271–3282, Aug 2013.
- [16] A. Levin, D. Lischinski, and Y. Weiss, “A closed-form solution to natural image matting,” *IEEE Transactions on Pattern Analysis and Machine Intelligence*, vol. 30, pp. 228–242, Feb 2008.
- [17] Q. Chen, D. Li, and C. Tang, “Knn matting,” *IEEE Transactions on Pattern Analysis and Machine Intelligence*, vol. 35, pp. 2175–2188, Sept 2013.
- [18] P. Lee and Y. Wu, “Nonlocal matting,” in *CVPR 2011*, pp. 2193–2200, June 2011.
- [19] L. Karacan, A. Erdem, and E. Erdem, “Alpha matting with kl-divergence-based sparse sampling,” *IEEE Transactions on Image Processing*, vol. 26, pp. 4523–4536, Sept 2017.
- [20] N. Hautière, J.-P. Tarel, D. Aubert, and Éric Dumont, “Blind contrast enhancement assessment by gradient ratioing at visible edges,” *Image Analysis Stereoology*, vol. 27, no. 2, pp. 87–95, 2011.